Real-time observations of water stable isotope dynamics during rainfall and throughfall events

Barbara Herbstritt, Benjamin Gralher, Markus Weiler

Hydrology, Faculty of Environment and Natural Resources, Albert-Ludwigs-University, Freiburg, 79098, Germany

Correspondence to: Barbara Herbstritt (barbara.herbstritt@hydrology.uni-freiburg.de)

Abstract. The water isotopic composition of throughfall is affected by complex diffusive exchange, evaporative enrichment of heavy isotopes, and mixing processes in the tree canopy. All interception processes occur simultaneously in space and time generating a complex pattern of throughfall depth and isotopic composition. This pattern ultimately cascades through the entire hydrologic system and is therefore crucial for isotope studies in catchment hydrology where recharge areas are often forested while reference meteorological stations are generally in the open. For the quasi real-time observation of the water isotopic composition ($\delta^{18}O$ and $\delta^{2}H$) of both gross precipitation and throughfall we developed an approach combining a membrane contactor (Membrana) with a laser-based Cavity Ring-Down Spectrometer (CRDS, Picarro), obtaining isotope readings every two seconds. A setup with two CRDS instruments in parallel analysing gross precipitation and throughfall simultaneously was used for the continuous observation of the temporal effect of interception processes. All devices were kept small to minimize dead volume and thereby, with time-lags of only four minutes for water from the rainfall collectors to the isotope analysers, to increase the temporal resolution of isotope observations. Complementarily, meteorological variables were recorded at high temporal resolution at the same location. The achieved evolution from discrete liquid or event-based bulk samples to continuous measurements allows for direct comparison with common meteorological measurements. This makes our approach a powerful tool towards more insight in the dynamic processes contributing to interception during rainfall events.

1 Introduction

Stable isotope ratios of water ($\delta^{18}O$ and $\delta^{2}H$) are ideal tracers due to the fact that they are part of the water molecule itself (Gonfiantini, 1986). They have proven to be powerful tools for the characterisation of water flow and transport processes with a long record of applications at different spatial and temporal scales and in all parts of the water cycle (Kendall and McDonnell, 1998; Vitvar et al., 2005). The isotopic composition of precipitation ultimately cascades through the entire hydrologic system affecting soil water, groundwater, evapotranspiration, and stream water isotopic signatures. Knowledge about the isotopic composition of precipitation is therefore crucial for isotope studies in catchment hydrology. . Many studies have used the temporal dynamics in the isotopic composition of precipitation for estimating catchment residence times, but especially in forested catchments, when meteorological and isotopic reference stations are in the open, interception losses

and accompanying isotope effects have a significant impact on the input function (Xu et al., 2014; Stockinger et al., 2015; Allen et al., 2017). The importance of understanding rainfall interception processes is presented in a thorough review by Allen et al. (2017). The reasons for the differences in amount and isotopic composition of gross precipitation (P_g) and throughfall (TF) are complex, since multiple interacting processes affect TF. They are driven by evaporation from the canopy during or between storms, diffusive exchange with ambient vapour, redistribution in the canopy, and storage effects where water is differentially retained or mixed. Also sub-canopy water recycling i.e. evapotranspiration and re-condensation (Green et al., 2015) as well as mixing with water from previous events (Allen et al., 2014) has been described. These effects reduced the mean depth and the difference in isotopic composition of event-based sampled TF compared to P_g. Depending on the species (spruce and beech) and on the density of the vegetation cover the volume weighted mean of the relative interception loss was in a range of 12% to 41%. It was typically higher for small events and generally led to enrichment of heavy isotopes in TF (Brodersen et al., 2000). However, ignoring the differences between P_g and TF depth results in an overestimation of the input amount to the system and would therefore be a source of error in hydrograph separation (Kubota and Tsuboyama, 2004) and other isotope related analyses. In ungauged catchments or when only P_g instead of TF data are available, isotopic correction factors were determined empirically (Stockinger et al., 2015; Calderon and Uhlenbrook, 2016) serving as surrogates to compensate for the lack of respective TF isotope data.

High spatial intra- and inter-storm variabilities have been found in depth and isotopic composition of TF. A synthesis study analysed the spatiotemporal variabilities of TF from 18 selected studies at a global scale. The study showed that the spatial patterns of TF, when related to leaf area index (LAI) as well as to spatial variability in general, were very heterogeneous and ecosystem dependent (Levia et al., 2011). Another study used a set of 94 TF collectors at three different forested sites, covering different types (coniferous and deciduous) and ages of trees, canopy densities and canopy diameters. There the authors investigated the spatial dependence of TF depth (storm-total) for three to seven storms in a six months period with a geostatistical approach finding a high spatiotemporal persistence (Keim et al., 2005). Recently, the observation of high spatial variability in collected TF stable isotopic compositions could be improved by using a set of roving collectors (Allen et al., 2015). Although hypothesized by the authors, intra- and inter-storm variabilities of TF amount did not necessarily correspond with variations in isotopic composition. Consequently, collecting representative TF input data for isotopes studies is still missing and an observational challenge (Allen et al., 2015).

Traditionally, the isotopic composition of liquid water is determined with discrete samples being analysed in the laboratory, hence conducting isotope studies always implied a trade-off between limited spatio-temporal resolution and extensive (and expensive) lab work. With the recent development of laser-based isotope analysers like off-axis integrated cavity output spectroscopy (OA-ICOS) or Cavity Ring-Down Spectroscopy (CRDS), there is now the possibility to analyse water stable isotopes faster and less expensive. The fact that water vapour is analysed directly ‘as water’ together with the field-deployability of the analysers and the virtually instant availability of isotope readings made way for several attempts aiming at in-situ isotope observations with high temporal resolutions. Berman et al. (2009) and Pangle et al. (2013) combined an autosampler with a flow-through system and were able to reveal otherwise unnoticed fine-scale (5-minutes) variations of

precipitation isotopic compositions. A commercially available VALCO® valve unit coupled with laser spectrometers for high-resolution sampling (9.5-minutes) was used by Leis et al. (2011) to investigate spring water isotope dynamics. Koehler and Wassenaar (2011) employed a marble-filled equilibrator and a minimodule device for producing and subsequently analysing a constant stream of vapour being in isotopic equilibrium with and therefore carrying in a known manner the isotopic information of the liquid phase of interest. Following the same principle, other researchers used gas-permeable ePTFE surgical tubings for the investigation of precipitation trajectories (Munksgaard et al., 2012a) or seawater-freshwater mixing ratios (Munksgaard et al., 2012b). For the continuous investigation of rapid water isotope changes in a soil column experiment, Herbstritt et al. (2012) employed a commercially available hydrophobic membrane contactor for converting a small fraction of liquid water continuously into a stream of vapour, which was directly analysed by the coupled isotope analyser. However, none of these approaches have attempted to observe rainfall and throughfall in parallel.

Recent interception studies, mostly based on bulk sampling data and focusing on spatial variations, are especially lacking an appropriate temporal resolution to be comparable with the available temporal resolution of meteorological input data and hence to describe and better understand the physics controlling the differences in isotopic composition between P_g and TF.

Therefore, the aim of this study is to develop an approach for the analysis of P_g and TF depth and isotopic composition at the point level at high temporal resolution based on the membrane contactor method, to compare and validate the continuous isotope measurements with discrete liquid samples as well as with event-based bulk samples. With this approach the dynamics in amount and isotopic composition of P_g and TF and hence, interception processes influencing amount and isotopic composition of TF can be investigated in unprecedented high temporal resolution.

2 Methods and Material

2.1 Sampling

We modified the setup developed and used previously for the in-situ observation of water stable isotopes in a soil column experiment (Herbstritt et al, 2012). A commercially available hydrophobic membrane contactor of 1 x 1 x 0.5 inch (MicroModule®, Membrana, Charlotte, NC, USA, www.liquicel.com) was combined with a CRDS isotope analyser (L2120-*i*, Picarro, Inc., Santa Clara, CA, USA, www.picarro.com). The contactor, originally designed for degassing liquids, was used in the so called 'sweep-mode' in order to continuously transform a small fraction of liquid water of interest with flowrates of 5-30 mL/min, according to manufacturer specifications, into a water vapour stream. Inside the contactor a microporous, hydrophobic, PP-based membrane (A = 100 cm²) divides the liquid from the gaseous phase. At the membrane's surface, dry carrier gas (e.g. N_2) mixes with vapour diffusing from the liquid phase through the pores across the membrane. Moist air then leaves the contactor at the gas outlet port (Fig. 1, right) which is directly connected to the CRDS. In the analyser-controlled stream of moist air (flow rate ~35 mL/min), readings of water vapour, $\delta^{18}O$ and $\delta^{2}H$ are given every two seconds. The method requires a thorough determination of the temperature to account for the temperature-dependent isotope fractionation factors of the membrane as described in detail by Herbstritt et al. (2012).

Several modifications of the original setup were made for the quasi real-time observation of water stable isotopes in rainfall. A standard rainfall collector was enlarged from 200 to 1810 cm² with a PP-funnel to ensure sufficient water flow in case of low rainfall intensities and also to account for small-scale spatial variabilities in TF. To protect against clogging by litter fall, a metal mesh with 1 x 1 mm covered the funnel. At the bottom end, a smaller funnel with a volume of 3 mL was installed. From there, a stream of water was pumped to the membrane contactor with a peristaltic pump at a constant flowrate of 5 mL/min while at the same time water exceeding this flowrate was spilled and collected via an additional funnel into a sampling bottle. This overflow was volume-weighted, contributing to the event-based bulk sample.

All connections were made by gas-tight PFA tubings with an inner diameter of 1 mm. Easily replaceable glass fibre syringe filters (pore size 1-2µm) were installed in line to protect the membrane contactor from clogging. Removal of smaller particles or biofilms inside the contactor could be facilitated by back flushing with deionized water as needed or periodical rinsing every 2 to 4 weeks with weak acids, respectively. Temperature of the water in the tubing just before the contactor was stabilized and kept constant at 16°C using a peltier element (UEPT-KIT3) and a controller (UR3274U5, both obtained from uwe electronic, Wachendorf, Germany, www.uweelectronic.de) to avoid super-saturation and condensation of the vapour on the way to the isotope analyser operated at room temperature. Vapour isotope data were recorded as soon as temperature and thus vapour concentration at the membrane contactor was stable, which was usually the case within 5 to 10 minutes after the onset of precipitation sampling. All tubings were kept as short as possible, facilitating a time shift of no more than four minutes between precipitation and the respective readings displayed by the isotope analyser (Fig. 1). During rainfall events, discrete liquid samples were taken every five minutes at the liquid outlet port of the membrane module and analysed later in the laboratory. The collected overflow plus excess water at the membrane module was volume-weighted and summed up to an event-based bulk sample. In close proximity (1.5 m) to the collector a tipping bucket (R3, Onset Rain Gauge) was installed. Rainfall was logged in 0.2 mm increments (HOBO UA-003-64 Pendant Event Data Logger, Onset, HOBO®, Bourne, MA, USA, www.onsetcomp.com) and data was aggregated to 1-minute intervals. Two of these setups were installed with 10 m horizontal distance from each other, sampling gross precipitation (P_g) and throughfall (TF) under a deciduous tree (*Acer campestre* L.) separately. In total, 28 bulk samples and nine continuously analysed events were obtained in August-September 2015 and throughout the vegetation period (May-September) of 2016. In any case, the measurements were carried out during the period when the leafs had reached their full sizes, in order to minimize the influence of the growing season. The meteorological variables air temperature (T_a) and relative humidity (RH) were recorded in 15 m distance to the tree with a CS215 sensor and logged with a CR1000 data logger (both available from Campbell Scientific, Inc., Logan, UT, USA, www.campbellsci.com) every minute. Additionally, the meteorological variables rainfall depth (P_g), air temperature (T_a), relative humidity (RH), air pressure, wind speed (v), and wind direction were available in 10 minute resolution from a climate station 250 m away.

Figure 1

2.2 Analyses

All isotope data are expressed in δ-notation calculated with the following equation:

$$\delta = \left(\frac{R_{sample}}{R_{VSMOW2}} - 1\right) * 1000‰ \quad (1)$$

where VSMOW2 is the Vienna Standard Mean Ocean Water and R is the isotope ratio ($^{18}O/^{16}O$ or $^{2}H/^{1}H$). Calibration of the samples was conducted using three in-house standards with distinct isotopic compositions, -16.65‰, -9.59‰, and 0.51‰ for $\delta\ ^{18}O$, -125.05‰, -66.50‰, and -2.40‰ for $\delta\ ^{2}H$, referenced to the international VSMOW-SLAP scale (Craig, 1961). They were pumped consecutively through the contactor after each rainfall event until a plateau in the isotope readings was reached (~10 minutes) and treated similar to the continuously sampled precipitation water. Hence, potential long-term changes of the membranes e.g. build-up of biofilms or mechanical changes (small cracks, fissures) at the membrane did not have an effect on calibrated isotope data. For data noise reduction of the continuous measurements we calculated moving averages with an integration time of 90 s. All liquid water samples were analysed on a CRDS laser spectrometer (Picarro L2130-*i*) with a post-calibration accuracy of ± 0.05‰ for $\delta\ ^{18}O$ and ± 0.35‰ for $\delta\ ^{2}H$.

D-excess (*d*) was used to indicate the deviation from the global meteoric water line (GMWL) and likely non-equilibrium fractionation by evaporation (Gat, 1996):

$$d = \delta^{2}H - 8 * \delta^{18}O \quad (2)$$

The difference in isotope characteristics between TF and P_g is indicated by the symbol Δ:

$$\Delta\delta^{18}O = \delta^{18}O_{TF} - \delta^{18}O_{Pg} \quad (3)$$

$$\Delta d = d_{TF} - d_{Pg} \quad (4)$$

Relative interception loss (*Loss*) is the difference in depth between P_g and TF

$$Loss = \frac{P_g - TF}{P_g} * 100\ \% \quad (5)$$

Vapour pressure deficit (VPD) is calculated to indicate potentially high or low evaporation with the following equation (modified from Foken, 2008):

$$VPD = 6.107hPa * e^{\left(\frac{17.62 * T_a}{243.12°C + T_a}\right)} * \left(1 - \frac{RH}{100\ \%}\right) \quad (6)$$

where RH is relative humidity in % and T_a is air temperature in °C.

3 Results

One example rainfall event observed in this study (Fig. 2) had a total depth of 6.8 mm and started with high rainfall intensities followed by more moderate intensities which lasted for roughly two hours. Continuous vapour derived stable isotope measurements, isotope ratios of discrete liquid and liquid bulk samples are shown for both isotope ratios investigated

to illustrate the increase of temporal information during one single rain event when analysing in high temporal resolution. The moving average of calibrated vapour derived data ranged between -5.45‰ and -7.53‰ for $\delta^{18}O$ and -27.36‰ and -45.64‰ for $\delta^{2}H$ with respective mean precisions of ± 0.26‰ and ± 1.53‰. Calibrated data of the liquid samples taken simultaneously were in a range of -5.34‰ to -7.43‰ in the case of $\delta^{18}O$ and -28.73‰ to -45.95‰ in the case of $\delta^{2}H$. Mean absolute deviation between the moving average of the continuously analysed vapour data and the discrete liquid samples was 0.11‰ and 1.35‰ with standard deviations of 0.096‰ and 0.81‰ for $\delta^{18}O$ and $\delta^{2}H$, respectively. The isotopic composition of the event-based bulk sample during this event was -5.68‰ for $\delta^{18}O$ and -32.67‰ for $\delta^{2}H$.

Figure 2

Analysing all 28 event-based bulk samples in this study, the variables rainfall depth (P_g), mean rainfall intensity, interception loss, $\delta^{18}O_{Pg}$, $\delta^{18}O_{TF}$, the difference in deuterium excess (Δd) and the isotopic difference $\Delta\delta^{18}O$ are correlated to each other in a scatterplot matrix (Fig. 3). A significant (p-value < 0.05) but moderate negative correlation between the logarithm of rainfall intensity and the relative interception loss indicates that the highest interception losses were found during events with lowest rainfall intensities. The interception loss ranges predominantly between 30% and 50%. Also a weak positive relationship between $\Delta\delta^{18}O$ and interception loss was found which means that the isotopic composition ($\delta^{18}O$) of precipitation when becoming throughfall is altered to a larger extent when interception losses are high. The isotopic composition of P_g ranges from -1.58‰ to -11.69‰ for $\delta^{18}O$ and is significantly correlated to the respective isotopic composition of TF which ranges from -0.88‰ to -10.15‰. Only non-significant correlations were found between the other investigated quantities. The explained variance by any of the considered variables alone was generally small.

Figure 3

In Figure 4 (a) the difference of the isotopic signature between TF and P_g ($\Delta\delta^{18}O$) of 28 bulk samples is shown. It was calculated from flux-weighted means of $\delta^{18}O$ of TF and P_g. The data of the bulk samples were grouped in classes of 0.5‰ increments. The maximum difference in $\delta^{18}O$ values of 2 - 2.5‰ was observed only for two events, while for 23 of the 28 events $\Delta\delta^{18}O$ was 1.5‰ or less. In contrast, in the shorter periods of continuous sampling, $\Delta\delta^{18}O$ values up to 3.5‰ were found (Table 1 and Fig. 4 (b). Each symbol in Figure 4 (b) indicates the mean difference in $\delta^{18}O$ (y-axis), whereas the length of the symbol indicates the duration of the continuous sampling (x-axis), including start and end time of the respective events. Two clusters can be identified with one containing three single rainfall events on a previously dry canopy, i.e. after at least 6 hours without rainfall, and the other containing six events on already wet canopies with markedly higher $\Delta\delta^{18}O$ values.

Table 1: Depth, intensity, and isotope values of continuously sampled P_g and TF. Data of differences in $\delta^{18}O$ ($\Delta\delta^{18}O$ (‰)) are reported as mean ± SD. (* tipping bucket malfunctioned)

			Rain (P_g)		Throughfall (TF)		TF-P_g differences	
Event #	Starting time	Duration (h:mm)	Depth (mm)	Intensity (mm/h)	Depth (mm)	Intensity (mm/h)	Loss (%)	$\Delta\delta^{18}O$ (‰)
1	2015/09/22 20:32	0:25	2.0	4.80	1.20	2.88	40.0	3.45 ± 1.16
2	2015/09/22 21:28	0:32	2.6	4.88	1.60	3.00	38.5	2.49 ± 0.98
3	2016/08/02 17:50	0:59	3.0	3.00	(6.20)*	6.20	(-106.7)	0.95 ± 0.37
4	2016/08/04 19:50	0:42	1.8	2.57	0.80	1.14	55.6	2.14 ± 0.5
5	2016/08/04 20:54	0:22	0.6	1.64	0.40	1.09	33.3	2.68 ± 0.27
6	2016/08/04 21:34	0:24	0.8	2.00	0.40	1.00	50.0	2.31 ± 0.26
7	2016/08/04 22:10	0:15	0.4	1.60	0.20	0.80	50.0	3.31 ± 0.35
8	2016/08/05 18:15	0:08	0.6	4.50	0.40	3.00	33.3	0.86 ± 0.32
9	2016/08/20 18:37	0:46	4.0	4.80	2.80	3.36	30.0	1.00 ± 0.33

Figure 4

Time series of (a) $\Delta\delta^{18}O$, (b) $\Delta\delta^{2}H$, and (c) Δd calculated from continuous isotope data of TF and P_g of all nine continuously observed events listed in Table 1 are illustrated in Figure 5. Values during events on initially dry canopies do not exceed 1.5‰ and 10‰ for $\Delta\delta^{18}O$ and $\Delta\delta^{2}H$, respectively, with Δd values ranging from +1‰ to -7‰. In contrast, values from events on wet canopies are in the range of +1.5‰ to +5‰ for $\Delta\delta^{18}O$ and +11‰ to +43‰ for $\Delta\delta^{2}H$ with Δd values ranging from +12‰ to -6‰.

Figure 5

The combination of collector funnel area (1810 cm²) and water flow rate (5 mL/min) resulted in a threshold rainfall intensity of 0.03 mm/min that was required to ensure an air bubble-free stream of water being pumped to the membrane contactor. Thus, periods of pure water flow at both (P_g and TF) contactors alternated with periods when air bubbles appeared at either one or both of the contactors in this example event (Fig. 6). Since the presence of bubbles proved to flaw isotope readings, calculations of $\Delta\delta^{18}O$, $\Delta\delta^{2}H$, and Δd were only reasonable for periods without bubbles at any contactor. The variability of the continuous P_g isotope data is higher than the variability of the continuous TF data, where the signal is more dampened over time. Relative to P_g, TF becomes increasingly enriched in heavy isotopes during the event. The variability of d is in the range of about 5‰ for both P_g and TF, fluctuating initially in a corridor between 10‰ and 15‰. However, d_{Pg} shows a

negative trend and decreases by about 10‰ over the course of the event whereas d_{TF} does not follow this trend and remains rather constant. Air temperature as well as vapour pressure deficit decrease with event duration.

Figure 6

4 Discussion

The modified setup of the method developed by Herbstritt et al. (2012) adapted to continuous rainfall and throughfall isotope measurement worked quite well in terms of providing continuous, thermo-regulated flows of water to the membrane modules and delivering reliable liquid water stable isotope data. The latter became evident by the good agreement of continuous measurements and single liquid samples (Fig. 2 and also Fig. 6) which was persistently in the order of the measurement uncertainty for both isotope ratios under investigation. Large intra-storm variabilities exist in the isotopic signature of P_g and TF, which would have been impossible to detect when solely relying on commonly taken event-based bulk samples or even on data representing a higher sampling interval of typically 5 mm precipitation depth. We found that the variability of the continuous P_g isotope data is higher than the variability of the continuous TF data (Fig. 6). For the latter, the signal is more dampened probably due to mixing processes, which was also found in other studies (Qu et al., 2013). The lower intensity and total depth of TF as compared to P_g is indicative for evaporation from the canopy. However, this is not reflected in continuous d_{TF} values (Fig. 6) which were expected to follow the trend of d_{Pg} values while being lower after evaporative non-equilibrium fractionation. The dynamics in the isotopic composition in P_g as well as in TF could be captured by the continuous measurements and also to some degree with the 5-minute discrete liquid samples. This provides a good evidence for the applicability of the developed continuous method. On the other hand, it is also an indication that a temporal resolution of around five minutes might be sufficient to capture the isotope dynamics of rainfall events, if continuous sampling is not possible. However, continuous data were instantly available whereas data of sampled liquid water were available not before conventional analysis via CRDS was completed, which lasted for another two days. In contrast, there is obviously a tremendous loss of information about short term dynamics or trends when comparing the results with commonly taken bulk samples or 5 mm depth incremented samples.

Depletion in heavy isotopes in open site rainfall was observed in the last ~30 minutes of the event presented in Figure 2. Several effects could cause such a pattern. The amount effect, reported for lower latitudes (Moore et al., 2014), can be ruled out due to the fact that at the same time rainfall intensity was quite low compared to other periods of this particular rainfall event. Also a rainout effect cannot be attributed to our data as it is only detectible on a spatial scale considering the movement of air masses and rain clouds. Rather, the simultaneous decrease of air temperature indicates the passing of a weather front which appears to be the relevant explanation for the observed changes in precipitation isotope values.

In the data of the collected bulk samples a significant negative correlation between interception loss and the meteorological variable rainfall intensity as well as a moderate negative correlation between relative interception loss and depth of incident rainfall could be observed (Fig. 3).This means that the highest interception losses were found during events with either lowest rainfall intensities or with lowest depths. A weak positive relationship also existed between $\Delta\delta^{18}O$ and interception loss, indicating that $\Delta\delta^{18}O$ increases with increasing interception losses. This is in line with results found in other studies (Dewalle and Swistock, 1994; Brodersen et al.; 2000, Keim et al.; 2005, Kato et al., 2013; Allen et al., 2017). Only non-significant correlations were found between the other investigated quantities. The small explained variance between any of the considered variables illustrates the complexity of the processes contributing to interception loss and the transformation of P_g isotope ratios when becoming TF.

Due to required minimum flowrates at the contactor (5 mL/min), the used setup with a collector area of 1810 cm² was limited to minimum rainfall intensities of 0.03 mm/min (1.8 mm/h). The fact that some of the investigated events appear to have intensities below 1.8 mm/h (Tab. 1) may be due to TF heterogeneities that came into effect at the different locations of the tipping bucket and TF sampling. For sampled intensities below the identified threshold value, a larger or multiple collectors would be necessary, whereby larger collection funnels in combination with low rainfall intensities will increase the risk of evaporative enrichment from the funnel surface, leading to methodological artefacts that need to be avoided. These effects, however, are typical for most throughfall collectors as large and long surfaces are preferred. Therefore, dimensioning the collectors always is a trade-off and the maximum size is limited.

Comparing $\Delta\delta^{18}O$ data during continuously measured events with those derived from event-based bulk samples, the differences are larger during the shorter continuously measured periods (Fig. 4). It should be noted that in this case the definition of a rainfall event is not consistent. Bulk samples cover the entire time period of rainfall regardless of intensity at the point of observation and mere existence of rainfall at the complementary observation point (P_g vs. TF). In contrast, continuous events are defined by sufficient simultaneous rainfall intensity at both points of observation due to our setups' properties. Therefore, natural rainfall events can only partially be captured by continuous synchronous observations. At the same time bulk samples represent the flux-weighted mean of all conditions constituting the respective event. Nonetheless, in the continuously analysed dataset two clusters could be distinguished representing rainfall on already wet and on initially dry canopies (Fig. 4 (b)). The fact that wet canopies lead to an even stronger enrichment in heavy isotopes can probably be attributed to partly evaporated and therefore isotopically enriched pre-event water that mixes with new rainfall water. This supports the interpretation that antecedent conditions have a clear impact on isotopic enrichment of TF which was also described in previous studies (Keim et al., 2005; Allen et al., 2014; Stockinger et al., 2015; Allen et al., 2017). Relative to P_g, TF becomes increasingly enriched in heavy isotopes (Fig. 6), which is similar to our observations of $\Delta\delta^{18}O$ in bulk samples on dry and wet canopies (Fig. 4 and Fig. 5). The additionally calculated Δd values did not show a clear or systematic pattern that would add to previous findings. Meteorological variables also did not provide a clear single evidence for the observed enrichment, indicating that multiple variables affect the isotopic processes in the canopy. Typically, air temperature as well

as vapour pressure deficit slightly decreased over the course of an event, but obviously evaporation still altered the isotopic signal as evidenced by the observed interception losses. At the same time mixing of antecedent water with new precipitation water occurred in the canopy. Therefore, it remains unclear to what extent the increase in difference between synchronous P_g and TF isotope data must be attributed to evaporative enrichment or to changing mixing processes following the variable rainfall intensities. Water redistribution in the canopy, i.e. movement of water to or from a specific place e.g. via flow along branches, may have an effect on the isotopic composition observed as it also changes the unknown spatial pattern of precipitation water isotopes. In addition, the spatial scale of mixing, certainly at the leaf level, but probably also among leafs as water drips from leaf to leaf, needs to be considered if we would like to decipher the isotope dynamics caused by water mixing and evaporation in the canopy of a tree.

The total number of observed events is lower in the case of the continuously measured events due to a number of events with rainfall intensities below the threshold for the continuous sampling method and due to several events during the night when the sampling setup was not operated. For continuous measurements the differences in the isotopic signature were consistently calculated from isochronic P_g and TF data although we are aware that water falling from the canopy (i.e. TF) is always a mixture of new rainfall (i.e. isochronic P_g) and rainfall that has occurred at different points in time before. The time lags depend on canopy storage capacity and rainfall intensity (Allen, 2017) and therefore vary within each single event as well as between different storms.

Highest $\Delta\delta^{18}O$ values were found in the cases of the continuous observations. One reason could be that the continuously analysed events are shorter and therefore potentially capturing extreme values while bulk samples represent flux-weighted mean isotopic signatures of the entire periods of rainfall and throughfall. On the other hand, we are aware that the calculation and interpretation of synchronous $\Delta\delta^{18}O$ and $\Delta\delta^{2}H$ data are disputable given assumable, yet unknown, time lags between P_g and TF. Within each rainfall event, also past trends and variabilities of the P_g isotopic compositions must be assumed to be reflected in instantaneous TF isotopic compositions, but are not considered with the proposed approach. However, a quite common intra-event P_g isotopic depletion trend (Fig. 2 and Fig. 6) combined with any positive time lag between P_g and TF would result in higher synchronous $\Delta\delta^{18}O$ values compared to estimates derived from bulk sample data.

For the quantitative description of processes affecting throughfall depth and isotopic composition, and thus the possible explanation for the discrepancies in $\Delta\delta^{18}O$ values, a mechanistic modeling approach could be envisioned. Such an approach could build on the one developed by Keim et al. (2006) and aim at the quantification of the intensity-dependent canopy storage capacity and hence variable time lags between P_g and TF. The canopy storage capacity has been shown to be a function of leaf area and rainfall intensity and may also depend on wind speed or other meteorological properties. While being attached to the canopy, water is exposed to meteorology-dependent, thus variable, evaporation. This causes the effective cumulative P_g depth to decrease thereby producing variable time lags or rather transit time distributions between P_g and TF. Evaporation also causes enrichment in heavy isotopes of canopy-stored water. Consequently, for every simulation time step the TF isotopic composition needs to be calculated consecutively taking into account the respective fractions of P_g

remaining from simultaneous and prior time steps and constituting the instantaneous reservoir releasing TF. In addition, internal mixing will occur at the leaf scale or inter-leaf scale. These mixing assumptions are probably least known and would need to be tested under different conditions. Finally, all relevant model parameters can be assumed to be dependent on meteorological variables thus further complicating this modeling and emphasizing the importance of continuous precipitation data representing different climates and vegetation characteristics.

5 Conclusions

We could demonstrate that the proposed method is suitable for continuously observing the stable water isotope dynamics in precipitation and throughfall. We facilitated a huge increase in temporal resolution compared to isotope assays based on bulk sampling. Our approach supersedes taking liquid samples and at the same time provides data much faster. The instant data availability enables immediate reactions during rainfall events while the operator is still in the field. Employing our setup, the temporal resolution of the isotope data corresponds with the temporal resolutions that are already common in high frequency meteorological observations.

All components employed in this study are commercially available and can be installed with reasonable effort. In the present design the setup cannot yet be left unattended due to the necessity of periodical cleaning and maintenance like changes of the in-line filters. However, proper precautions excluding clogging by e.g. leaf debris should solve this issue as well. We are therefore confident that our setup, especially when employed across larger spatial scales, will contribute to the aim of thorough isotopic sampling of TF, which is crucial in hydrological studies in particular for forested sites but also for other vegetated areas.

Due to the selected dimensions of our setup and the resulting minimum rainfall intensity of 0.03 mm/min, the system was not able to capture events with low rainfall intensities, e.g. most stratiform rainfall events, but this can be changed to make the approach suitable for a wider range of rainfall intensities. The lack of strong correlations between the investigated rainfall characteristics illustrates the complexity of interception processes. Especially, knowledge about intra-canopy mixing and the time lags between P_g and TF as required for a precise, physically based calculation of the evaporative enrichment still remains a challenge for future applications.

Acknowledgements

We gratefully thank our technician Emil Blattmann for technical assistance. The article processing charge was funded by the German Research Foundation (DFG) and the University of Freiburg in the funding programme Open Access Publishing. We thank three anonymous reviewers for their constructive comments which helped to improve the manuscript.

References

Allen, S. T., Brooks, J. R., Keim, R. F., Bond, B. J., and McDonnell, J. J.: The role of pre-event canopy storage in throughfall and stemflow by using isotopic tracers, Ecohydrology 7, doi: 10.1002/eco.1408, 2014

Allen, S. T., Keim, R. F., and McDonnell, J. J.: Spatial patterns of throughfall isotopic composition at the event and seasonal timescales, J Hydrol 522, 58–66, doi: 10.1016/j.jhydrol.2014.12.029, 2015

Allen, S. T., Keim, R. F., Barnard, H. R., McDonnell, J. J., and Renée Brooks, J.: The role of stable isotopes in understanding rainfall interception processes: a review, Wiley Interdiscip Rev Water 4, e1187. doi: 10.1002/wat2.1187, 2017

Berman, E. S. F., Gupta, M., Gabrielli, C., Garland, T., and McDonnell, J. J.: High-frequency field-deployable isotope analyzer for hydrological applications, Water Resour Res 45,W10201, doi: 10.1029/2009wr008265, 2009

Brodersen, C., Pohl, S., Lindenlaub, M., Leibundgut, C., and Wilpert, K. v.: Influence of vegetation structure on isotope content of throughfall and soil water, Hydrol Process 14, 1439–1448, doi: 10.1002/1099-1085(20000615)14:8<1439::AID-HYP985>3.0.CO;2-3, 2000

Calderon, H. and Uhlenbrook, S.: Characterizing the climatic water balance dynamics and different runoff components in a poorly gauged tropical forested catchment, Nicaragua, Hydrol Sci J 61, 2465–2480, doi: 10.1080/02626667.2014.964244, 2016

Craig, H.: Standards for reporting concentrations of deuterium and oxygen-18 in natural waters, Science 133, 3467, 1961

Dewalle, D.R., Swistock, B.R., 1994. Differences in oxygen-18 content of throughfall and rainfall in hardwood and coniferous forests. Hydrol. Process. 8, 75–82. doi.org/10.1002/hyp.3360080106

Foken, T.: Micrometeorology, Springer-Verlag, doi: 10.1007/978-3-540-74666-9, 2008

Gat, J. R.: Oxygen and hydrogen isotopes in the hydrologic cycle, Annu Rev Earth Planet Sci 24, 225–262, doi: 10.1146/annurev.earth.24.1.225, 1996

Gonfiantini, R.: Environmental Isotopes in Lake Studies, in: Fontes J.-Ch. and Fritz, P. (eds.): Handbook of Environmental Isotope Geochemistry, Elsevier, Amsterdam, 113–168, 1986

Green, M. B., Laursen, B. K., Campbell, J. L., McGuire, K. J., and Kelsey, E. P.: Stable water isotopes suggest sub-canopy water recycling in a northern forested catchment, Hydrol Process 29, 5193–5202, doi: 10.1002/hyp.10706, 2015

Herbstritt, B., Gralher, B., and Weiler, M.: Continuous in situ measurements of stable isotopes in liquid water. Water Resour Res 48:W03601, doi: 10.1029/2011wr011369, 2012

Kato, H., Onda, Y., Nanko, K., Gomi, T., Yamanaka, T., Kawaguchi, S., 2013. Effect of canopy interception on spatial variability and isotopic composition of throughfall in Japanese cypress plantations. J. Hydrol. 504, 1–11. doi.org/10.1016/j.jhydrol.2013.09.028

Keim, R. F., Skaugset, A. E., and Weiler, M..: Temporal persistence of spatial patterns in throughfall, J Hydrol 314, 263–274, doi: https://doi.org/10.1016/j.jhydrol.2005.03.021, 2005

Keim, R.F., Skaugset, A.E., Weiler, M.: Storage of water on vegetation under simulated rainfall of varying intensity. Adv.

Water Resources 29, 974–986, 2006

Kendall, C. and McDonnell, J. J.: Isotope tracers in catchment hydrology, Elsevier Science, Amsterdam, New York, 1998

Koehler, G. and Wassenaar, L. I.: Realtime Stable Isotope Monitoring of Natural Waters by Parallel-Flow Laser Spectroscopy, Anal Chem 83, 913–919, doi: 10.1021/ac102584q, 2011

Kubota, T. and Tsuboyama, Y.: Estimation of evaporation rate from the forest floor using oxygen-18 and deuterium compositions of throughfall and stream water during a non-storm runoff period, J For Res 9, 51–59, doi: 10.1007/s10310-003-0054-y, 2004

Leis, A., Plieschnegger, M., Harum, T., Stadler, H., Schmitt, R., Pelt, A.v., and Zerobin, W.: Isotope Investigations at an Alpine Karst Aquifer by Means of On-Site Measurements with High Time Resolution and Near Real-Time Data Availability, in: International Symposium in Isotopes in Hydrology, Marine Ecosystems and Climate Change Studies, 2011

Levia, D. F., Keim, R.F., Carlyle-Moses, D.E., and Frost, E.E.: Throughfall and Stemflow in Wooded Ecosystems, in: Forest Hydrology and Biogeochemistry, Springer-Verlag, 425-443, 2011

Moore, M., Kuang, Z., Blossey, P.N.: A moisture budget perspective of the amount effect, Geophys Res Lett 41, 1329-1335, doi: 10.1002/2013GL058302, 2014

Munksgaard, N. C., Wurster, C. M., Bass, A., and Bird, M. I.: Extreme short-term stable isotope variability revealed by continuous rainwater analysis, Hydrol Process 26, 3630–3634, doi: 10.1002/hyp.9505, 2012a

Munksgaard, N. C., Wurster, C. M., Bass, A., Zagorskis, I., and Bird, M. I.: First continuous shipboard δ18O and δD measurements in sea water by diffusion sampling-cavity ring-down spectrometry, Environ Chem Lett 10, 301–307, doi: 10.1007/s10311-012-0371-5, 2012b

Pangle, L. A., Klaus, J., Berman, E. S. F., Gupta, M., and McDonnell, J. J.: A new multisource and high-frequency approach to measuring δ2H and δ18O in hydrological field studies, Water Resour Res 49, 1-7, doi: 10.1002/2013wr013743, 2013

Qu, S., Zhou, M., Shi, P., Liu, H., Bao, W., Chen, X., 2014. Differences in oxygen-18 and deuterium content of throughfall and rainfall during different flood events in a small headwater watershed. Isotopes Environ. Health Stud. 50, 52–61. https://doi.org/10.1080/10256016.2014.845565

Stockinger, M. P., Lücke, A., McDonnell, J. J., Diekkrüger, B., Vereecken, H., and Bogena, H. R.: Interception effects on stable isotope driven streamwater transit time estimates, Geophys Res Lett 42, 5299–5308, doi: 10.1002/2015GL064622, 2015

Vitvar, T., Aggarwal, P., and McDonnell, J. J.: A Review of Isotope Applications in Catchment Hydrology, in: Aggarwal P., Gat J. R., Froehlich K. F. (eds.): Isotopes in the Water Cycle, Springer, Dordrecht, 2005

Xu, X., Guan, H., and Deng, Z.: Isotopic composition of throughfall in pine plantation and native eucalyptus forest in South Australia, J Hydrol 514, 150–157, doi: http://dx.doi.org/10.1016/j.jhydrol.2014.03.068, 2014

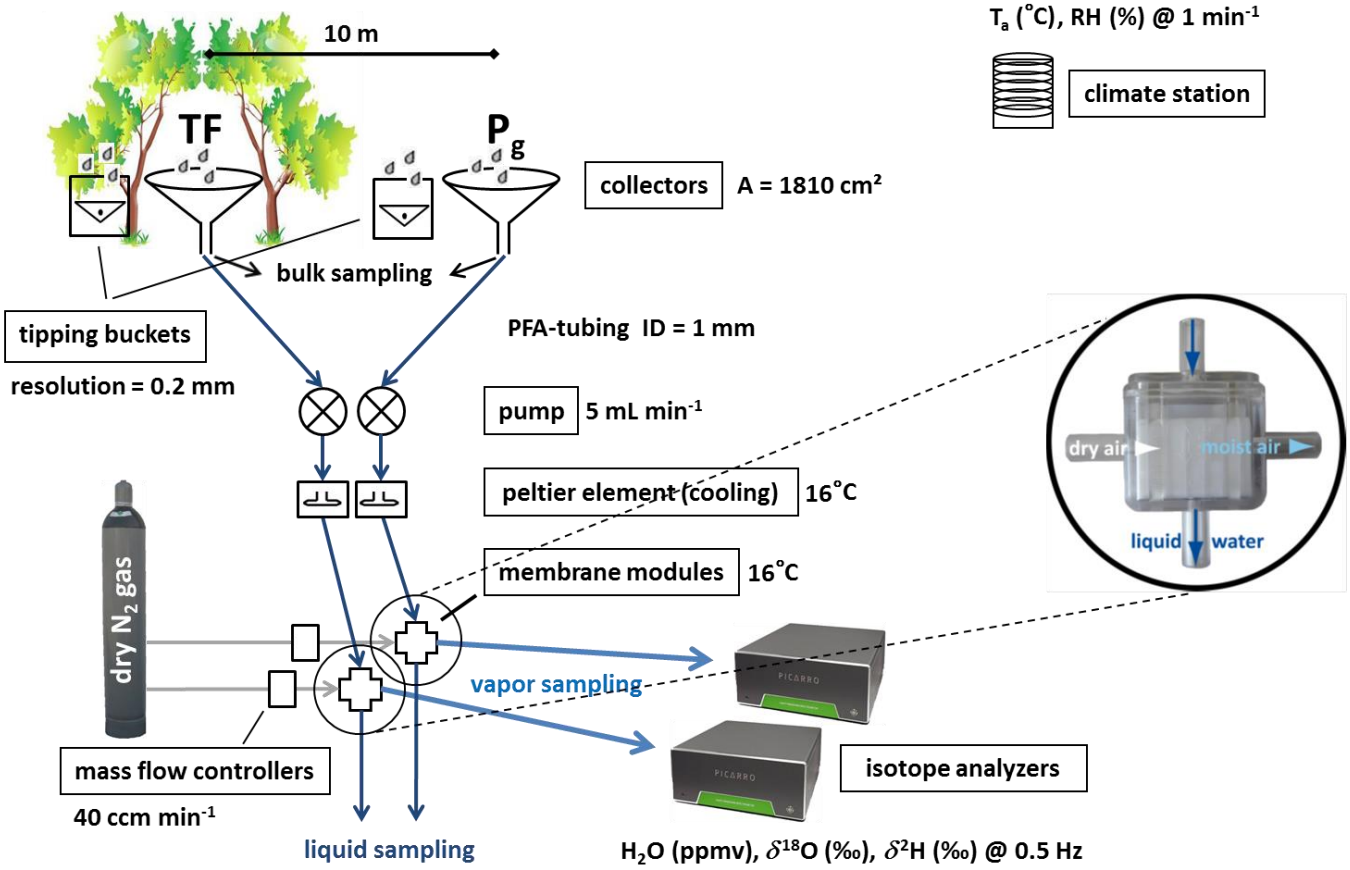

Figure 1: Setup for continuous water vapour stable isotope measurements of gross precipitation (P_g) and throughfall (TF) with two analyzers in parallel; membrane contactor (center-right) employed for continuous production of water vapour; discrete liquid and liquid bulk sampling of P_g and TF; recording of rainfall depth (tipping buckets, upper left) and the meteorological variables T_a and RH (upper right) every minute.

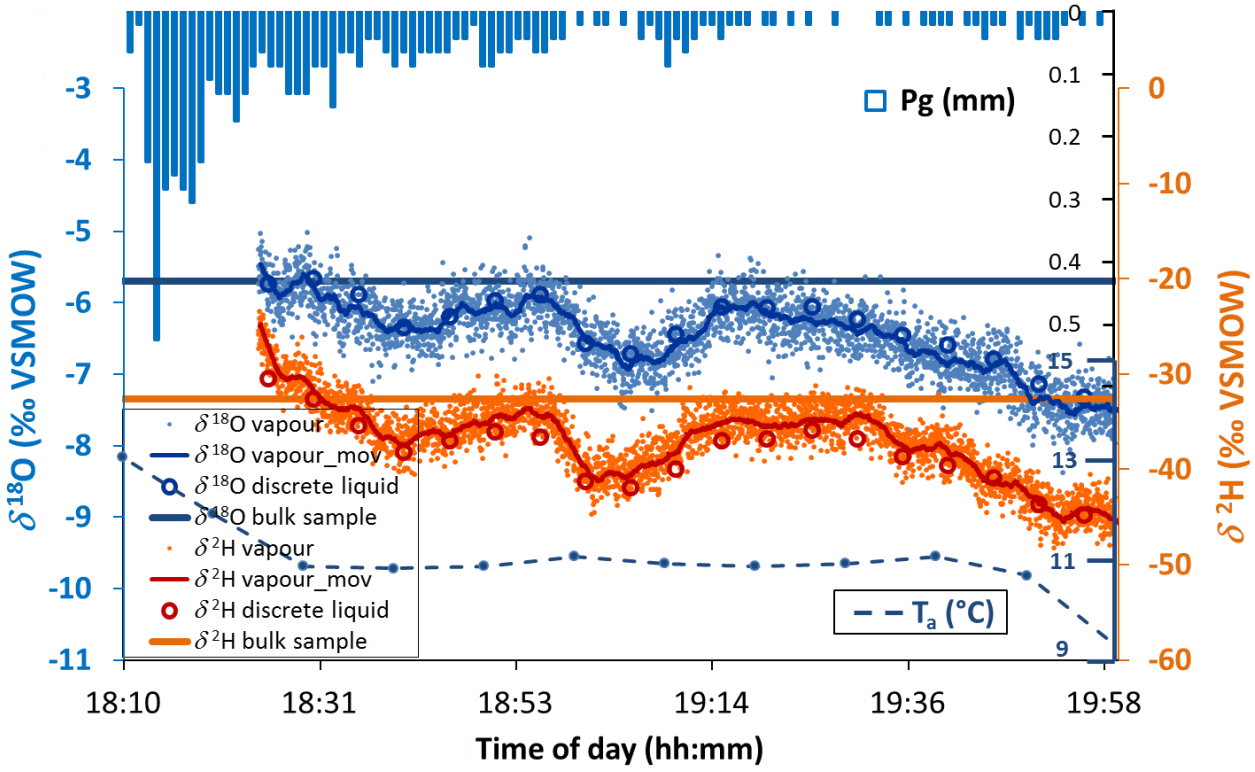

Figure 2: Time series of rainfall (P_g) depth per minute (vertical bars); 10-minute data of air temperature (T_a) (dashed line) during the rainfall event from April 17th 2015; data of $\delta^{18}O$ in blue and $\delta^{2}H$ in orange; vapour-derived data recorded every two seconds (small dots), starting after temperature at the contactor was stable, 90 sec. moving average (solid lines), discrete liquid samples (open circles) taken every five minutes, event-based bulk sample (horizontal bars).

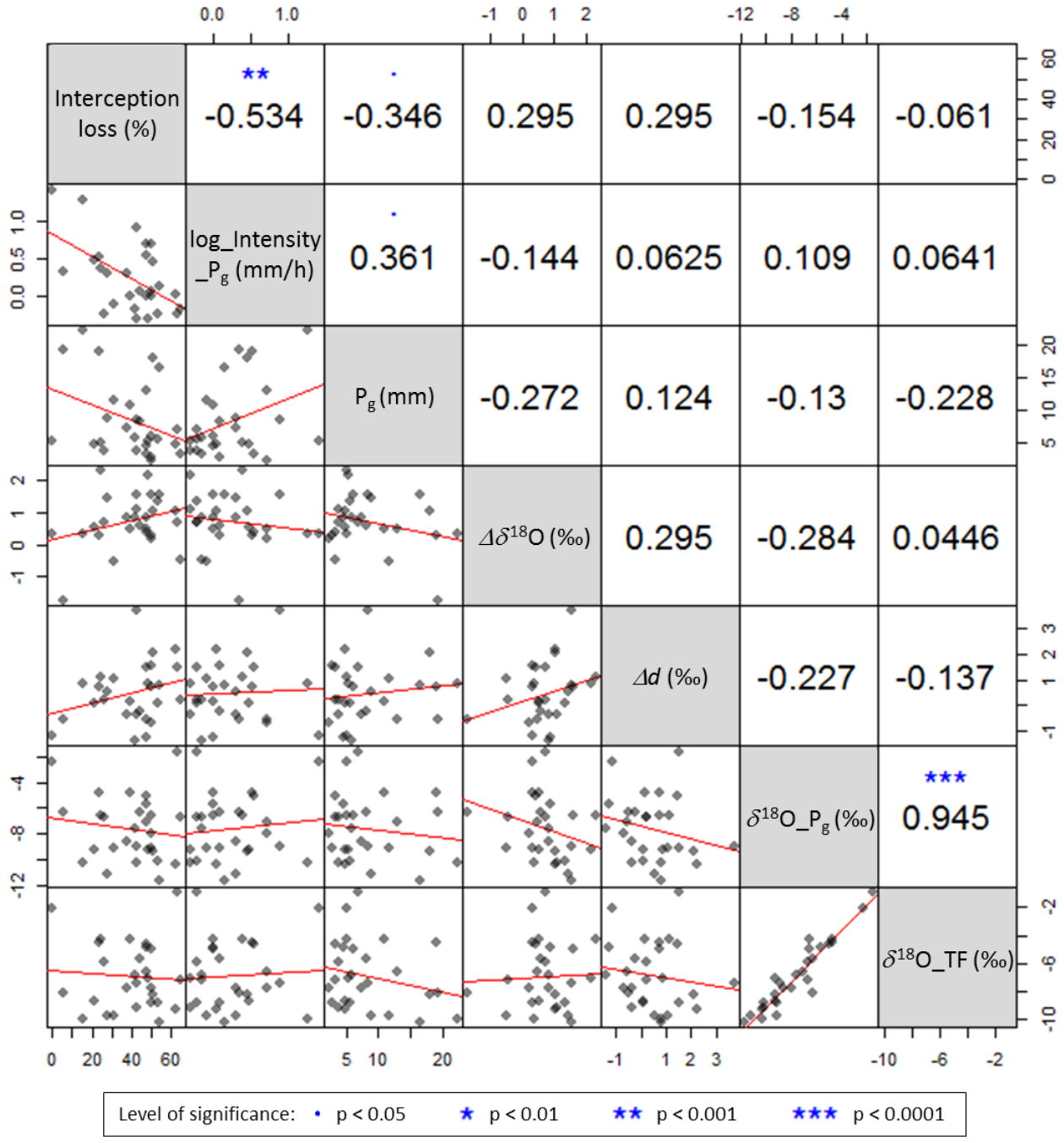

Figure 3: Scatter plot matrix of depths- and isotope-related characteristics derived from 28 event-based bulk samples. Upper right part: Pearson correlation coefficients and level of significance (stars); lower left part: scatter plots and linear regressions (red lines).

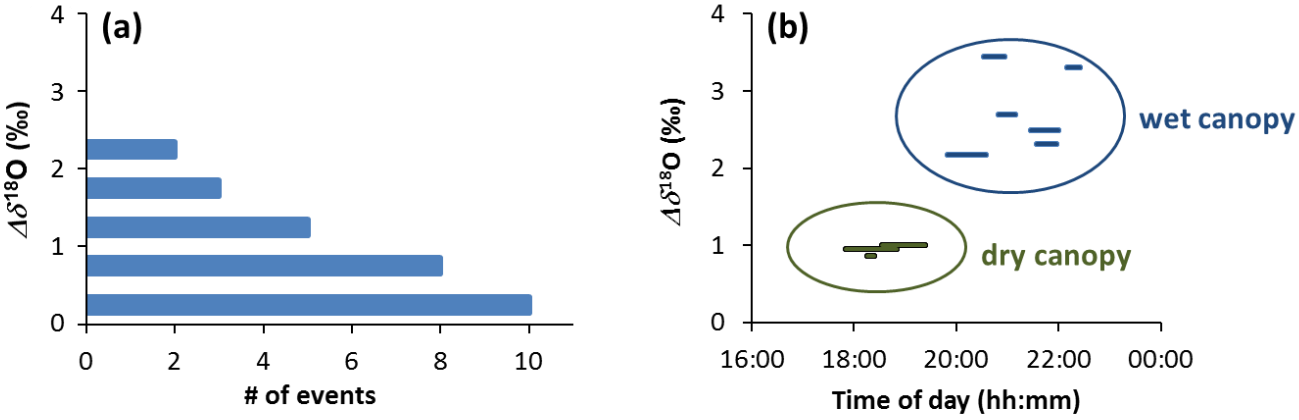

Figure 4: Difference of the isotopic signature ($\Delta\delta^{18}O$) between TF and P_g for (a) 28 event-based bulk samples and (b) 9 continuously analysed events of the same period.

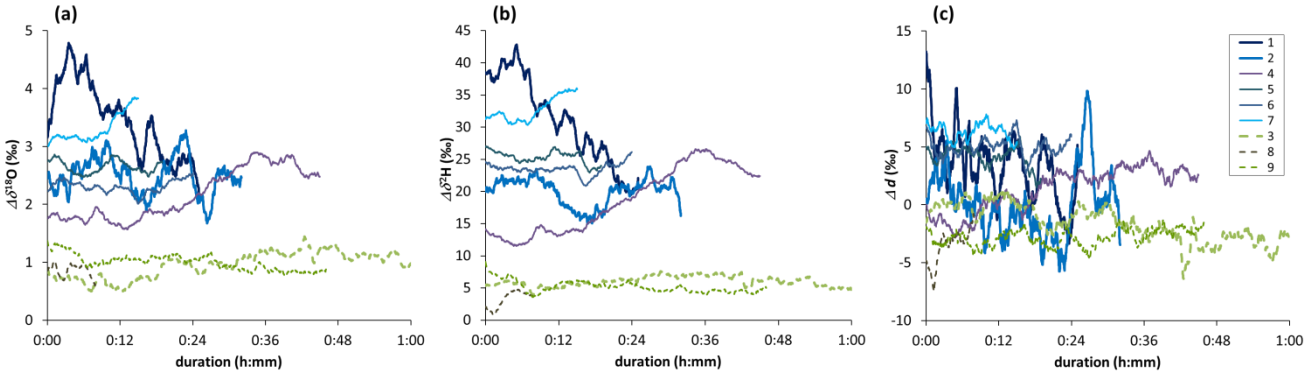

Figure 5: Time series of deviations of isotopic signature between TF and P_g, (a) $\Delta\delta^{18}O$, (b) $\Delta\delta^{2}H$, (c) Δd; events on initially dry canopy (dashed line) and on wet canopy (solid lines).

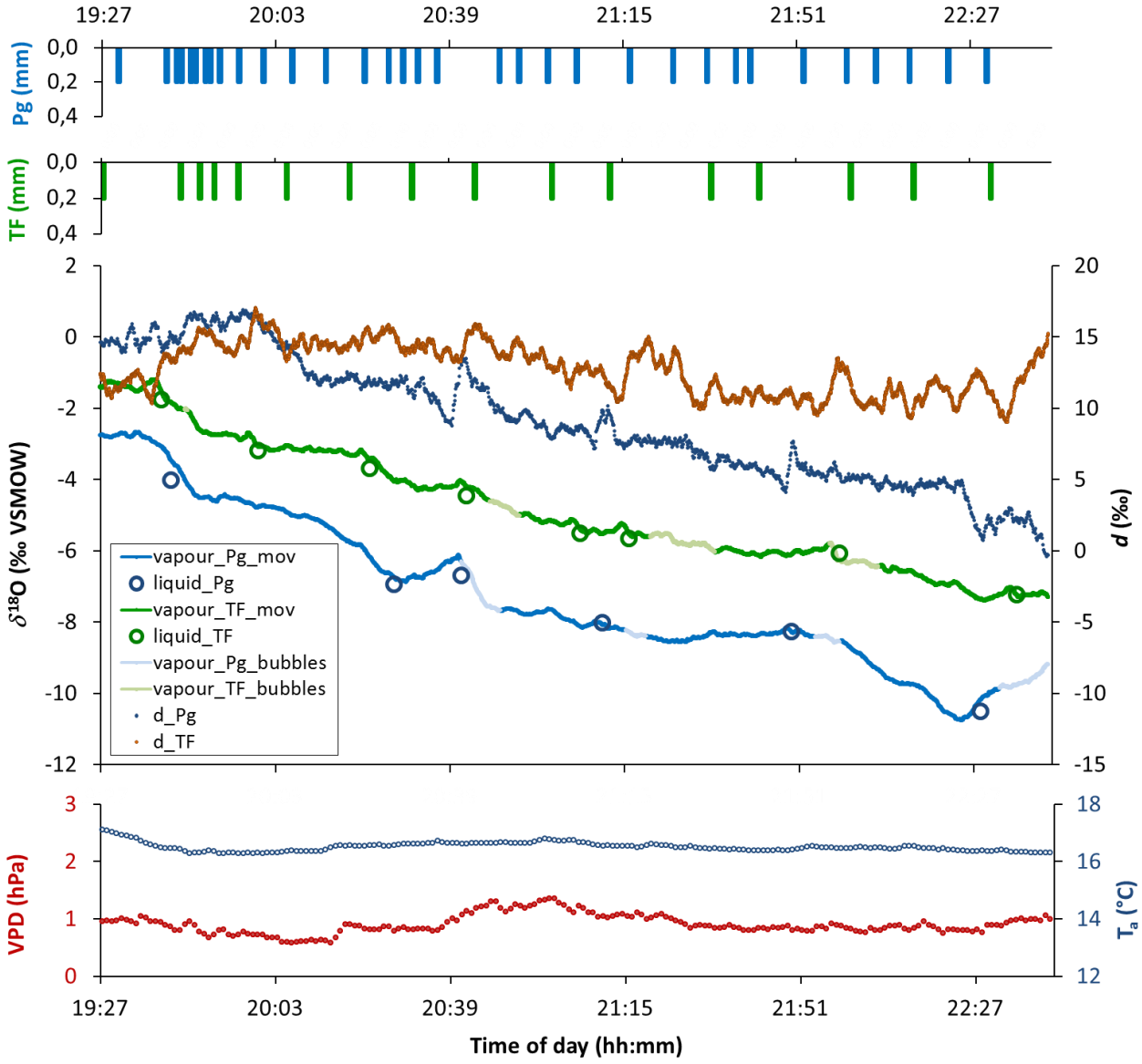

Figure 6: Time series of $\delta^{18}O$ and d derived from vapour sampling of P_g (blue) and TF (green), discrete liquid samples (big circles), air temperature (T_a) (small blue circles) and vapour pressure deficit (VPD) (red) of the rainfall event from August 4th 2016. Time series of d_{Pg} (dark blue dots), d_{TF} (brown dots) and T_a are referenced on the right vertical axes. Periods of intensities below threshold for the continuous sampling method (bubbles at membrane contactor) are shown in light blue (P_g) and light green (TF).